Figure 1. Flow diagram and Kaplan–Meier estimates of *de novo* activation of HBV after LDLT

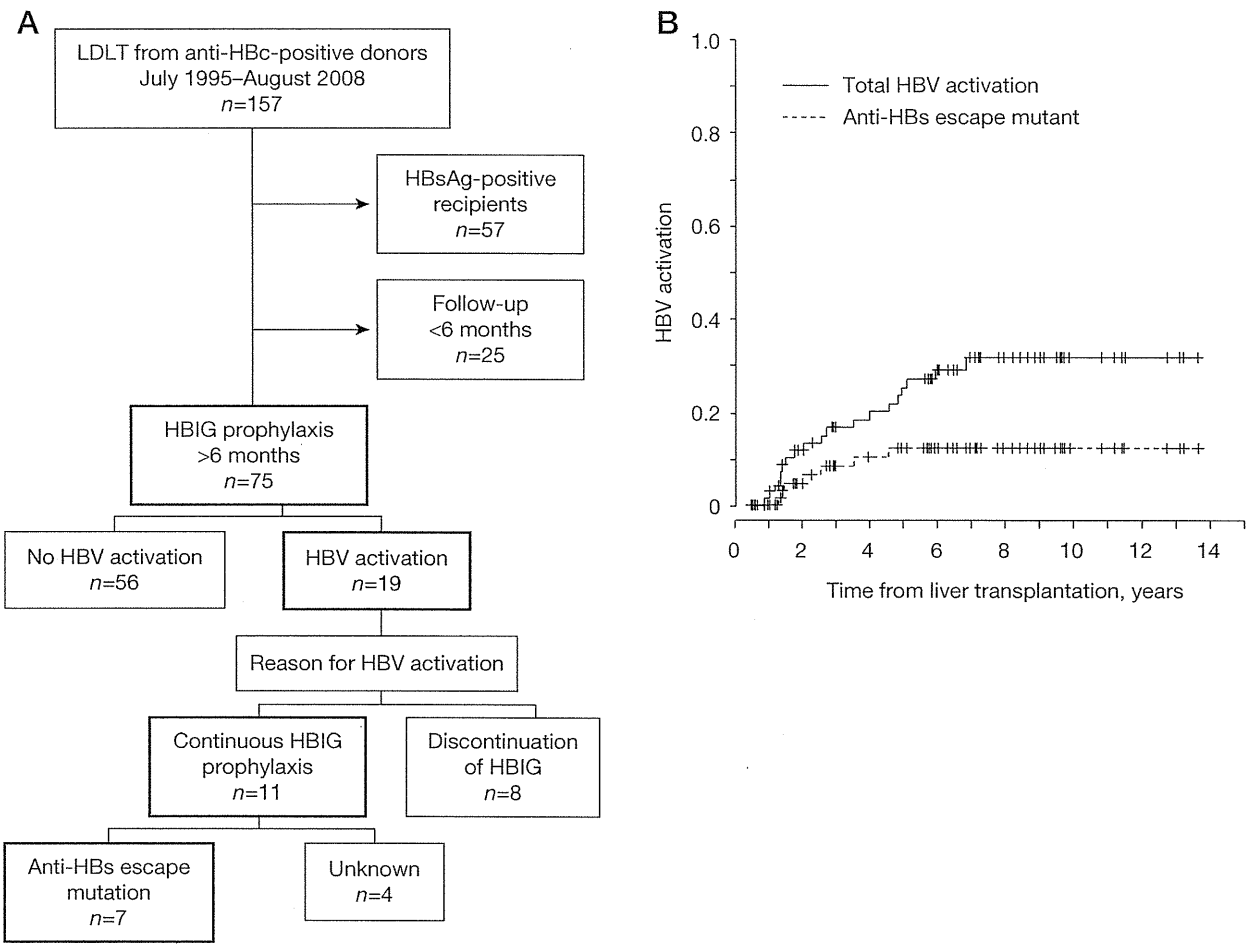

(A) Flow diagram showing *de novo* activation of HBV after living donor liver transplantation (LDLT) from hepatits B core antibody (anti-HBc)-positive donors. (B) Kaplan–Meier estimates of the rate of patients who showed *de novo* activation of HBV after LDLT from anti-HBc-positive donors. The total rate and rate of activation of HBV with hepatitis B surface antibody (anti-HBs) escape mutations are shown. HBIG, hepatitis B immunoglobulin; HBsAg, hepatitis B surface antigen.

are given, and the data were analysed by the χ^2 test. The rates of patients who showed HBV activation after LDLT were estimated using the Kaplan–Meier method. $P<0.05$ was considered significant.

Results

De novo activation of HBV in recipients from anti-HBc-positive donors

Among the 75 recipients who received HBIG prophylaxis >6 months after LDLT with liver grafts from anti-HBc-positive donors, 19 (25%) patients developed *de novo* activation of HBV (Figure 1A). The rate of HBV activation estimated by the Kaplan–Meier method was 3% at 1 year, 17% at 3 years, 25% at 5 years, and 29% at 10 years (Figure 1B). Of the 19 recipients with HBV activation, 8 had HBV activation due to transient discontinuation of HBIG (Figure 1A). In the remaining 11 patients with HBV activation, despite continuous HBIG prophylaxis, the emergence of HBV with anti-HBs escape mutations was confirmed in 7 patients, including 2 patients who were described in our previous report [13]. The rate of *de novo* activation of HBV with anti-HBs escape mutations estimated by the Kaplan–Meier method was 8% at 3 years and 12% at 5 years (Figure 1B). The other four recipients, in whom the reason for HBV activation was unknown, were previously reported by us [13].

Clinical features of patients with *de novo* activation of HBV with anti-HBs escape mutations

To clarify the characteristics of patients with *de novo* activation of HBV with anti-HBs-escape mutations, the clinical features of recipients with HBV with anti-HBs escape mutations ($n=7$) were listed and compared

Table 1. Clinical features of patients with *de novo* activation of HBV with anti-HBs escape mutation, of those without HBV activation after liver transplantation and also of donors

Characteristic	Activation of HBV with anti-HBs escape mutations (n=7)	No HBV activation (n=56)	P-value
Recipient			
Age, years	17 (0–67)	12 (0–62)	0.433[a]
Male/female	3/4	21/35	1.000[b]
Primary disease			
Cholestatic diseases	4 (57)	31 (55)	–
Hepatocellular diseases	0	8 (14)	–
Neoplastic diseases	1 (14)	6 (11)	–
Acute liver failure	0	1 (2)	–
Metabolic diseases	0	3 (5)	–
Retransplantation	1 (14)	6 (11)	–
Other	1 (14)	1 (2)	–
HBV markers before LDLT			
Anti-HBs-positive	3 (43)	18 (32)	0.677[b]
Anti-HBe-positive	0	7 (13)	0.581[b]
Anti-HBc-positive	0	17 (30)	0.175[b]
Donor			
Age, years	42 (34–55)	45 (24–65)	0.200[a]
Male/female	3/4	31/25	0.694[b]
Anti-HBs-positive	7 (100)	44 (79)	0.329[b]
Anti-HBe-positive	4 (57)	38 (68)	0.419[b]
Follow-up period, months	86 (48–151)	94 (12–180)	0.646[a]

Qualitative variables are displayed as n (%) and quantitative variables expressed as median (range) for non-normally distributed variables. [a]Wilcoxon rank-sum test. [b]χ^2 test. Anti-HBc, heptatitis B core antibody; anti-HBe, hepatitis B e antibody; anti-HBs, hepatitis B surface antibody; LDLT, living donor liver transplantation.

Table 2. Clinical features of seven patients with *de novo* activation of HBV with anti-HBs escape mutation after liver transplantation

Patient number	Age, years[a]	Sex	Months from LDLT to HBV activation	Anti-HBs titre before HBV activation, IU/l	At the time of HBV activation			
					Anti-HBs titre, IU/l	HBsAg, COI	Serum HBV DNA, copies/ml	Peak ALT, IU/l
1	12	F	16.8	418.4	275.2	>2,000	$>10^{7.6}$	410
2	22	M	54.9	27.8	16.6	60.4	$10^{6.6}$	1,300
3	26	F	17.9	284.5	82.6	10.2	$>10^{7.6}$	81
4	70	F	42.2	44.0	17.9	668.8	$10^{7.1}$	204
5	59	M	24.1	188.8	105.4	21.3	$10^{3.5}$	131
6	18	F	30.6	96.9	157.4	6.9	$10^{4.5}$	153
7	2	M	15.7	218.8	74.3	187.3	NE	111

[a]Age at HBV activation. ALT, alanine aminotransferase; anti-HBs, hepatitis B surface antibody; COI, cutoff index; F, female; HBsAg, hepatitis B surface antigen; LDLT, living donor liver transplantation; M, male; NE, not examined.

with those of recipients without HBV activation (n=56; Table 1). The two groups of patients did not differ significantly by age, sex or serological markers for HBV before LDLT with regard to either recipients or donors. Of note, all seven patients with *de novo* activation of HBV with anti-HBs escape mutations were negative for anti-HBc pre-operatively, and no anti-HBc-positive recipients (n=17) developed *de novo* activation of HBV.

The details of the clinical features of the seven patients who developed *de novo* activation of HBV with anti-HBs-escape mutations are summarized in Table 2. In the seven patients, serum HBsAg and HBV DNA became positive 15.7–54.9 months (median 24.1 months) after LDLT. Serum anti-HBs titres were maintained at 27.8–418.4 IU/l before HBV activation by HBIG administration. At the time of HBV activation, all patients were positive for anti-HBs, despite being positive for serum HBV DNA and HBsAg, when *de novo* hepatitis B was diagnosed. The genotype of HBV in all seven patients was C, which is the major genotype in Japan [25]. All patients showed high serum ALT levels. Five of the seven patients received tacrolimus only for immunosuppression at the time of HBV activation, patient number 3 had tacrolimus with

prednisolone and mycophenolate mofetil, and patient number 4 received cyclosporine and prednisolone.

Sequence analysis of serum HBV DNA

Results of the sequence analysis of serum HBV DNA in these seven patients are shown in Figure 2. We focused our analysis on the immunodominant loop encompassing amino acid (aa) 101–163 of the S protein, which includes the 'a' determinant region (aa 124–147), the major target of neutralizing anti-HBs antibodies due to its exposure at the surface of viral particles [14,16,26]. Sequencing of the S gene revealed the presence of mutations in the immunodominant loop in all patients. These mutations within the S protein led to G145A substitution in patient number 1, G145R substitution in patients numbered 2, 3, 4, 6 and 7, and Q129P substitution in patient number 5 (Figure 2B). The mutations at aa 145 or aa 129 in HBsAg are known to be escape mutations from anti-HBs [9,16,18,22]. Several other mutations with amino acid substitutions, whose roles have not yet been clarified, were found at aa 101, aa 103, aa 110, aa 113, aa 114, aa 120, aa 126, aa 143, aa 155 and aa 161.

Treatment for *de novo* activation of HBV with anti-HBs escape mutations

Entecavir treatment (0.5 mg) was started for four patients (numbers 1–4) immediately after the diagnosis of *de novo* activation of HBV with anti-HBs-escape mutations. After the administration of entecavir, serum HBsAg and HBV DNA promptly decreased and became undetectable at 2.5, 3.3, 6 and 2.5 months after the start of entecavir treatment, respectively (Figure 3 and Table 3). Serum ALT levels also decreased in association with the decrease in serum HBV DNA. After confirming the stable negativity of HBsAg, entecavir treatment was stopped in three patients (numbers 1–3) at 5.8, 5.9 and 9.9 months after beginning the treatment, respectively. Thereafter, serum HBsAg and HBV DNA remained negative during the follow-up periods of 22.2, 24.7 and 20.6 months after withdrawal of entecavir, respectively (Table 3). Entecavir administration was continued for patient number 4 at the time of the analysis for this study because the patient wanted to continue the treatment. Patients numbered 5 and 6 received early administration of lamivudine after the diagnosis of *de novo* activation of HBV. However, they did not achieve serum HBV clearance by 26.6 and 4.6 months, respectively, at which time adefovir was added. Even after treatment with a combination of lamivudine and adefovir for 33.2 months, patient number 5 remained chronically HBsAg-positive. In patient number 6, serum HBsAg and HBV DNA became negative at 9.5 months after adefovir administration. Patient number 7 who did not receive nucleoside analogue treatment for hepatitis B developed chronic hepatitis B as confirmed by liver histology.

Discussion

In this report, we demonstrated the clinical features of *de novo* activation of HBV with anti-HBs-escape mutations under HBIG prophylaxis after liver transplantation. The rate of *de novo* activation of HBV with anti-HBs escape mutations was 12% at 5 years. No significant difference of baseline characteristics between patients with *de novo* activation of HBV with anti-HBs-escape mutations and patients without HBV activation was identified, but all patients who had activation of anti-HBs escape mutant HBV were pre-operatively anti-HBc-negative. Early entecavir treatment was very effective for patients with *de novo* activation of HBV with anti-HBs escape mutations and the treatment induced complete clearance of serum HBsAg and HBV DNA and resulted in sustained negativity for HBsAg even after the termination of entecavir treatment.

Two reasons for *de novo* activation of HBV after LDLT from anti-HBc-positive donors were revealed in this study: discontinuation of HBIG and emergence of an anti-HBs escape mutant. However, the reason for *de novo* HBV activation in four patients is still unknown. HBV activation by HBIG discontinuation is preventable by careful follow-up to reduce non-compliance of HBIG use. The most important reason for HBV activation is emergence of anti-HBs escape mutations under HBIG prophylaxis, because it is unpredictable and difficult to prevent. In the present study, no anti-HBc-positive patients developed *de novo* activation of HBV with anti-HBs-escape mutations. The reason for this is also unknown, but we expect that individuals with resolved hepatitis B have memory T-cells and various antibodies for HBV, including antibodies against PreS1 and PreS2 as well as anti-HBs, and the T-cells and antibodies could inhibit the proliferation of HBV with anti-HBs-escape mutations.

A characteristic serological feature at the onset of *de novo* activation of HBV with anti-HBs-escape mutations was positivity of anti-HBs at the time of HBV DNA appearance in the serum. Because anti-HBs cannot bind HBsAg that has anti-HBs escape mutations [16], HBV will increase even in the presence of anti-HBs. Therefore, we must be cautious to the development of hepatitis B due to HBV with anti-HBs-escape mutations, even when serum anti-HBs titre is maintained at a high level by HBIG administration. A regular evaluation of serum HBsAg and/or HBV DNA is recommended. Duration from liver transplantation to activation of anti-HBs-escape mutants were 15.7–54.9 months in this study. The previous study reported that activation of HBV with

Figure 2. DNA and amino acid sequences from seven patients with anti-HBs escape mutations

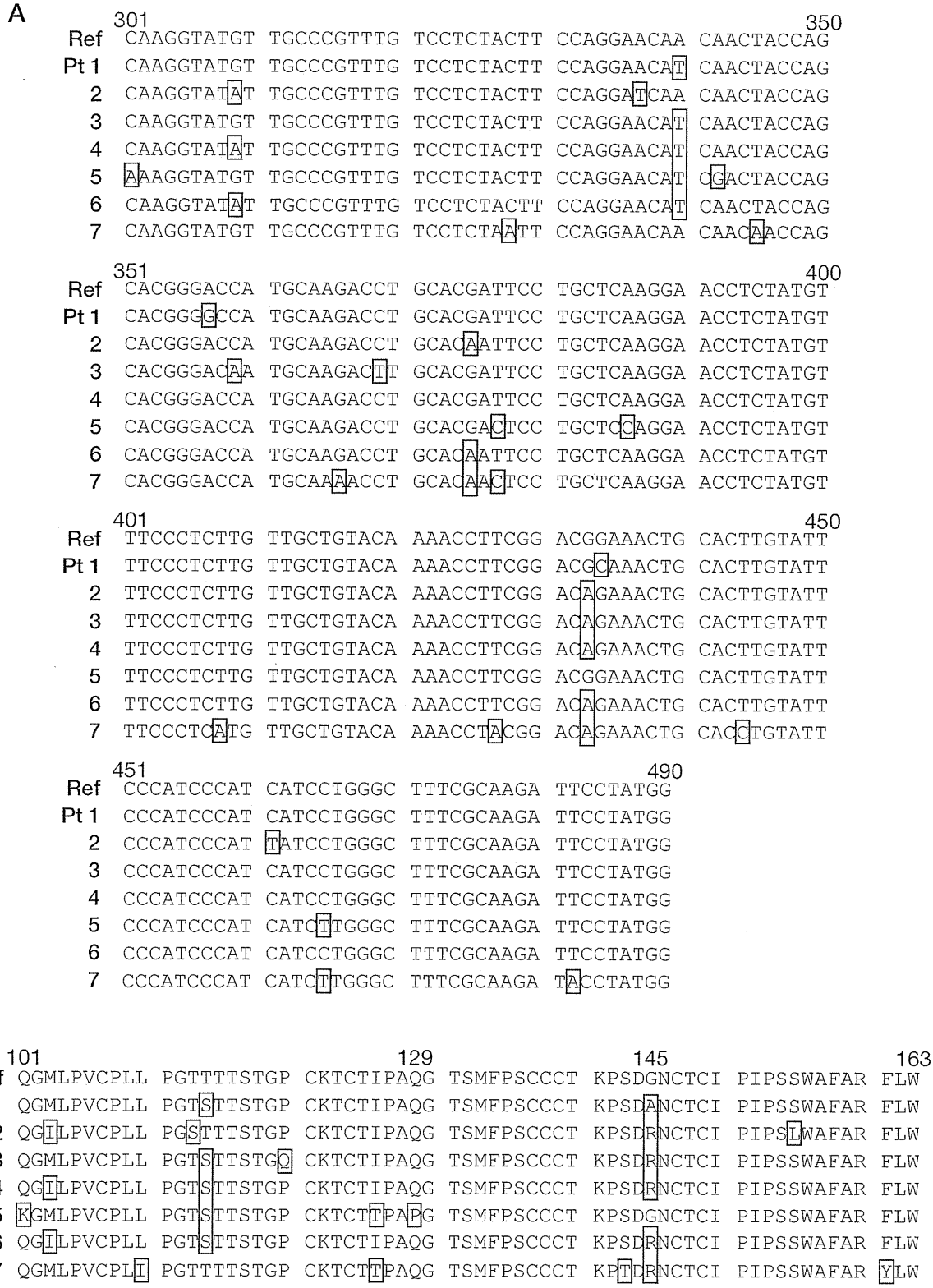

(A) DNA sequences between nucleotide 301 and 490 of the S gene and (B) amino acid sequences between positions 101 and 163 of the S protein of HBV from seven patients (Pt) with hepatitis B surface antibody (anti-HBs) escape mutations. The sequences are aligned with HBV genotype C (subtype adr) reference sequence (Ref; AB033550 [32]). Boxes indicate the positions showing differences from the Ref.

Figure 3. Clinical course of four patients who received entecavir treatment for *de novo* activation of HBV with anti-HBs escape mutations

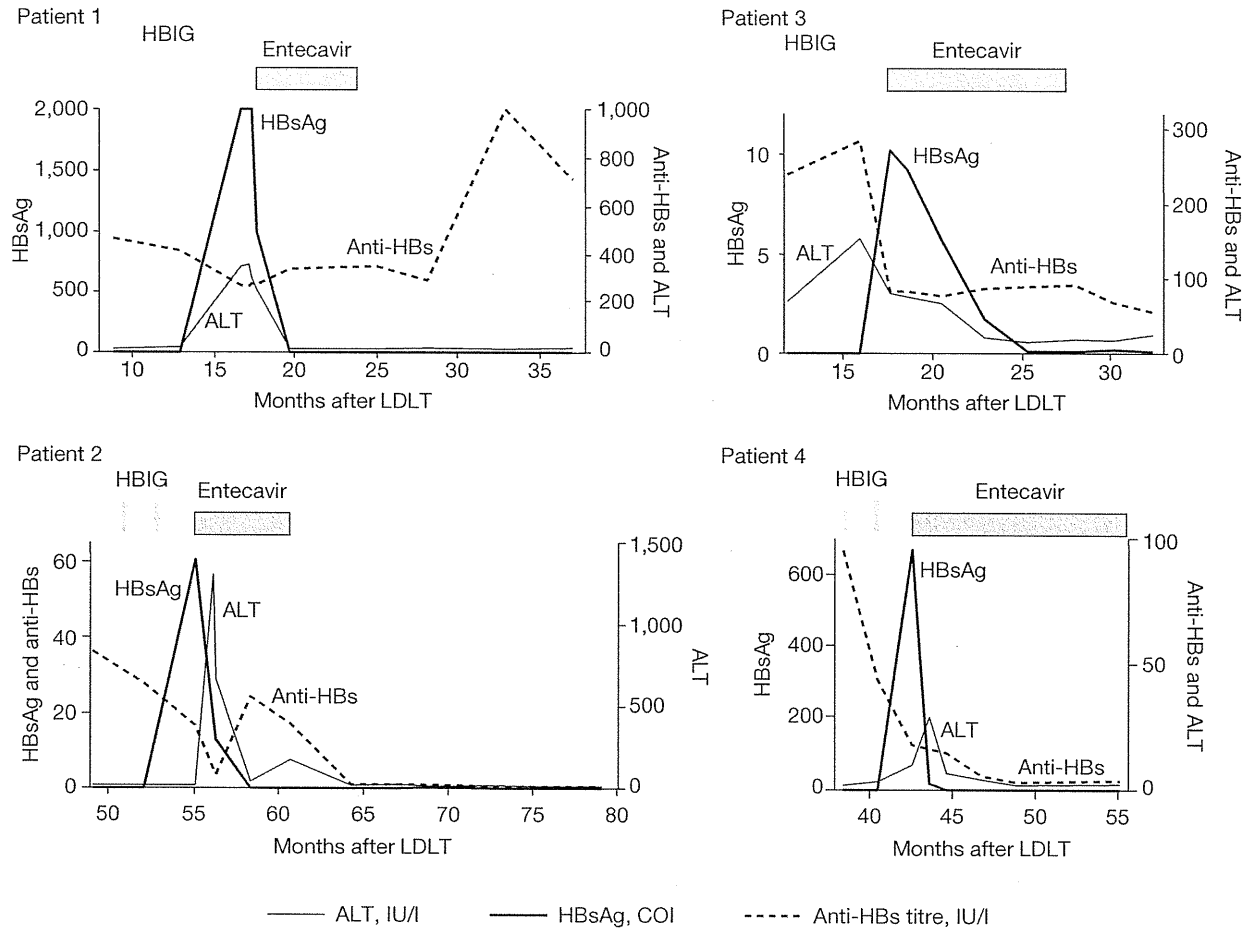

The administration of hepatitis B immunoglobulin (HBIG) is shown as arrows, and treatments with entecavir are indicated as shaded boxes. ALT, alanine aminotransferase; anti-HBS, hepatitis B surface antibody; COI, cutoff index; HBsAg, hepatitis B surface antigen; LDLT, living donor liver transplantation.

anti-HBs-escape mutations in HBsAg-positive recipients occurred 1–20 months after liver transplantation [22]. According to these results, the regular evaluation of HBV should be initiated just after liver transplantation and continued for the patient's lifetime.

The natural clinical course after *de novo* activation of HBV without nucleoside analogue treatment has been revealed in previous reports. We reported on a total of 19 cases of *de novo* activation of HBV after LDLT [7,13] without treatment after HBV activation. Overall, 16 of the 19 (84%) recipients, including 1 patient with anti-HBs escape mutant HBV, became HBsAg carriers; 1 died of fibrosing cholestatic hepatitis and only 2 patients spontaneously resolved to an HBsAg-negative state. Similar results showing that a majority of patients suffering from *de novo* activation of HBV after liver transplantation developed liver cirrhosis or chronic hepatitis have been reported [5,6,27]. These results indicate that most patients with *de novo* activation of HBV after liver transplantation enter an HBsAg carrier state without anti-HBV treatment because of the immunosuppressive conditions. Therefore, an effective management strategy is required for patients with *de novo* activation of HBV after liver transplantation.

We recently reported the beneficial effects of short-term lamivudine treatment for *de novo* activation of HBV caused by reasons other than anti-HBs escape mutations [13]. Lamivudine administration during the acute phase of *de novo* activation of HBV resulted in complete clearance of HBsAg from the serum in five of six patients, and all five remained negative for HBsAg even after the termination of lamivudine treatment. However, as shown in the present study, clearance of

Table 3. Treatment for seven patients with *de novo* activation of HBV with anti-HBs escape mutation after liver transplantation

Patient number	Treatment	Present status	Follow-up period after HBV activation, months	Duration from initiation of NA to disappearance of HBsAg, months	Duration of NA treatment, months	Present treatment
1	Entecavir	Resolved	28.0	2.5	5.8	None
2	Entecavir	Resolved	30.6	3.3	5.9	None
3	Entecavir	Resolved	30.5	6	9.9	None
4	Entecavir	Resolved	18.9	2.5	18.9	Entecavir
5	Lamivudine plus adefovir	Chronic hepatitis	59.8	–	59.8	Lamivudine plus adefovir
6	Lamivudine plus adefovir	Resolved	67.8	14.1	67.8	Adefovir
7	None	Chronic hepatitis	125.1	–	–	None

Anti-HBs, hepatitis B surface antibody; HBsAg, hepatitis B surface antigen; NA, nucleoside analogue.

HBsAg was not achieved in two patients with HBV with anti-HBs escape mutation by lamivudine administration. Although one patient achieved clearance of HBsAg after administration of adefovir, another patient developed chronic hepatitis B despite adding adefovir. In contrast, we demonstrated here the potent efficacy of entecavir on HBV with anti-HBs-escape mutations. The reason for the difference in efficacy between lamivudine and entecavir is unclear. Recent reports indicate that the overlap of the gene encoding HBsAg by the polymerase gene creates a unique situation in which a change within the polymerase gene following nucleoside analogue treatment might result in structural changes in the HBsAg protein and a subsequent reduction in the antigenicity of the protein. Lamivudine-resistant mutations in the polymerase gene are, indeed, associated with changes in the HBsAg protein, with a consequent reduction in antigenicity of the HBsAg protein comparable to that of anti-HBs-escape mutants [28,29]. The reverse might also be true. It has been reported that anti-HBs-escape mutations can produce a functionally significant alteration in the viral polymerase and influence the viral replication phenotype [30]. Both entecavir and lamivudine are nucleoside analogues that inhibit the HBV polymerase, but the mechanism of inhibition is different between these two nucleoside analogues. Entecavir inhibits HBV replication at three different steps: the priming of HBV DNA polymerase, reverse transcription of the negative-strand HBV DNA from the pregenomic RNA, and synthesis of the positive-strand HBV DNA, whereas lamivudine lacks the effect of the priming of HBV DNA polymerase [31]. The difference in the mechanism of HBV polymerase inhibition between entecavir and lamivudine may contribute to the difference in the efficacy of each nucleoside analogue on HBV with anti-HBs-escape mutations.

In conclusion, escape mutations from anti-HBs caused *de novo* activation of HBV under HBIG prophylaxis after liver transplantation from donors with resolved hepatitis B. Early administration of entecavir is important to avoid the subsequent development of acute liver failure or chronic hepatitis caused by *de novo* activation of HBV with anti-HBs-escape mutants.

Acknowledgements

This work was supported by Grants-in-aid for Scientific Research from the Ministry of Education, Culture, Sports, Science and Technology, and the Ministry of Health, Labor and Welfare of Japan.

Disclosure statement

The authors declare no competing interests.

References

1. Bréchot C, Thiers V, Kremsdorf D, Nalpas B, Pol S, Paterlini-Brechot P. Persistent hepatitis B virus infection in subjects without hepatitis B surface antigen: clinically significant or purely 'occult'? *Hepatology* 2001; 34:194–203.
2. Michalak TI, Pasquinelli C, Guilhot S, Chisari FV. Hepatitis B virus persistence after recovery from acute viral hepatitis. *J Clin Invest* 1994; 93:230–239.
3. Marusawa H, Uemoto S, Hijikata M, *et al.* Latent hepatitis B virus infection in healthy individuals with antibodies to hepatitis B core antigen. *Hepatology* 2000; 31:488–495.
4. Umeda M, Marusawa H, Seno H, *et al.* Hepatitis B virus infection in lymphatic tissues in inactive hepatitis B carriers. *J Hepatol* 2005; 42:806–812.
5. Chazouillères O, Mamish D, Kim M, *et al.* 'Occult' hepatitis B virus as source of infection in liver transplant recipients. *Lancet* 1994; 343:142–146.
6. Dickson RC, Everhart JE, Lake JR, *et al.* Transmission of hepatitis B by transplantation of livers from donors positive for antibody to hepatitis B core antigen. The National Institute of Diabetes and Digestive and Kidney Diseases Liver Transplantation Database. *Gastroenterology* 1997; 113:1668–1674.
7. Uemoto S, Sugiyama K, Marusawa H, *et al.* Transmission of hepatitis B virus from hepatitis B core antibody-positive donors in living related liver transplants. *Transplantation* 1998; 65:494–499.

8. Roque-Afonso AM, Feray C, Samuel D, *et al.* Antibodies to hepatitis B surface antigen prevent viral reactivation in recipients of liver grafts from anti-HBC positive donors. *Gut* 2002; 50:95–99.
9. Shouval D, Samuel D. Hepatitis B immune globulin to prevent hepatitis B virus graft reinfection following liver transplantation: a concise review. *Hepatology* 2000; 32:1189–1195.
10. Cholongitas E, Papatheodoridis GV, Burroughs AK. Liver grafts from anti-hepatitis B core positive donors: a systematic review. *J Hepatol* 2010; 52:272–279.
11. Saab S, Waterman B, Chi AC, Tong MJ. Comparison of different immunoprophylaxis regimens after liver transplantation with hepatitis B core antibody-positive donors: a systematic review. *Liver Transpl* 2010; 16:300–307.
12. Dodson SF, Bonham CA, Geller DA, Cacciarelli TV, Rakela J, Fung JJ. Prevention of *de novo* hepatitis B infection in recipients of hepatic allografts from anti-HBc positive donors. *Transplantation* 1999; 68:1058–1061.
13. Umeda M, Marusawa H, Ueda M, *et al.* Beneficial effects of short-term lamivudine treatment for *de novo* hepatitis B virus reactivation after liver transplantation. *Am J Transplant* 2006; 6:2680–2685.
14. Ashton-Rickardt PG, Murray K. Mutants of the hepatitis B virus surface antigen that define some antigenically essential residues in the immunodominant a region. *J Med Virol* 1989; 29:196–203.
15. Carman WF. The clinical significance of surface antigen variants of hepatitis B virus. *J Viral Hepat* 1997; 4 Suppl 1:11–20.
16. Waters JA, Kennedy M, Voet P, *et al.* Loss of the common 'a' determinant of hepatitis B surface antigen by a vaccine-induced escape mutant. *J Clin Invest* 1992; 90:2543–2547.
17. Carman WF, Zanetti AR, Karayiannis P, *et al.* Vaccine-induced escape mutant of hepatitis B virus. *Lancet* 1990; 336:325–329.
18. Hsu HY, Chang MH, Liaw SH, Ni YH, Chen HL. Changes of hepatitis B surface antigen variants in carrier children before and after universal vaccination in Taiwan. *Hepatology* 1999; 30:1312–1317.
19. Kohno H, Inoue T, Tsuda F, Okamoto H, Akahane Y. Mutations in the envelope gene of hepatitis B virus variants co-occurring with antibody to surface antigen in sera from patients with chronic hepatitis B. *J Gen Virol* 1996; 77:1825–1831.
20. Yamamoto K, Horikita M, Tsuda F, *et al.* Naturally occurring escape mutants of hepatitis B virus with various mutations in the *S* gene in carriers seropositive for antibody to hepatitis B surface antigen. *J Virol* 1994; 68:2671–2676.
21. Carman WF, Trautwein C, van Deursen FJ, *et al.* Hepatitis B virus envelope variation after transplantation with and without hepatitis B immune globulin prophylaxis. *Hepatology* 1996; 24:489–493.
22. Ghany MG, Ayola B, Villamil FG, *et al.* Hepatitis B virus S mutants in liver transplant recipients who were reinfected despite hepatitis B immune globulin prophylaxis. *Hepatology* 1998; 27:213–222.
23. Karthigesu VD, Allison LM, Fortuin M, Mendy M, Whittle HC, Howard CR. A novel hepatitis B virus variant in the sera of immunized children. *J Gen Virol* 1994; 75:443–448.
24. Lok AS, McMahon BJ. Chronic hepatitis B. *Hepatology* 2007; 45:507–539.
25. Yoshikawa A, Gotanda Y, Suzuki Y, *et al.* Age- and gender-specific distributions of hepatitis B virus (HBV) genotypes in Japanese HBV-positive blood donors. *Transfusion* 2009; 49:1314–1320.
26. Waters JA, Brown SE, Steward MW, Howard CR, Thomas HC. Analysis of the antigenic epitopes of hepatitis B surface antigen involved in the induction of a protective antibody response. *Virus Res* 1992; 22:1–12.
27. Roche B, Samuel D, Gigou M, *et al. De novo* and apparent *de novo* hepatitis B virus infection after liver transplantation. *J Hepatol* 1997; 26:517–526.
28. Sloan RD, Ijaz S, Moore PL, Harrison TJ, Teo CG, Tedder RS. Antiviral resistance mutations potentiate hepatitis B virus immune evasion through disruption of its surface antigen a determinant. *Antivir Ther* 2008; 13:439–447.
29. Torresi J, Earnest-Silveira L, Deliyannis G, *et al.* Reduced antigenicity of the hepatitis B virus HBsAg protein arising as a consequence of sequence changes in the overlapping polymerase gene that are selected by lamivudine therapy. *Virology* 2002; 293:305–313.
30. Torresi J, Earnest-Silveira L, Civitico G, *et al.* Restoration of replication phenotype of lamivudine-resistant hepatitis B virus mutants by compensatory changes in the 'fingers' subdomain of the viral polymerase selected as a consequence of mutations in the overlapping *S* gene. *Virology* 2002; 299:88–99.
31. Seifer M, Hamatake RK, Colonno RJ, Standring DN. *In vitro* inhibition of hepadnavirus polymerases by the triphosphates of BMS-200475 and lobucavir. *Antimicrob Agents Chemother* 1998; 42:3200–3208.
32. Okamoto H, Tsuda F, Sakugawa H, *et al.* Typing hepatitis B virus by homology in nucleotide sequence: comparison of surface antigen subtypes. *J Gen Virol* 1988; 69:2575–2583.

Accepted 12 October 2010; published online 12 April 2011

Full Length

Arthritis & Rheumatism
DOI 10.1002/art.34318

The Pattern-Recognition Receptor NOD1 Promotes Production of Inflammatory Mediators in Rheumatoid Arthritis Synovial Fibroblasts

Kazuhiro Yokota[1], MD, Takashi Miyazaki[2], PhD, Hossein Hemmatazad[1], MD, Renate E. Gay[1], MD, Christoph Kolling[3] MD, Ursula Fearon[4], PhD, Hiromichi Suzuki[2,5], MD, Toshihide Mimura[6] MD, Steffen Gay[1], MD, Caroline Ospelt[1], MD

[1]Center of Experimental Rheumatology, University Hospital Zurich and Zurich Center of Integrative Human Physiology (ZIHP), University of Zurich, Switzerland

[2]Community Health Science Center, Saitama Medical University, Saitama, Japan

[3]Schulthess Clinic, Zurich, Switzerland

[4]Department of Rheumatology, Dublin Academic Medical Centre and The Conway Institute of Biomolecular and Biomedical Research, Dublin 4, Ireland

[5]Department of Nephrology, Faculty of Medicine, Saitama Medical University, Saitama, Japan

[6]Department of Rheumatology and Applied Immunology, Faculty of Medicine, Saitama Medical University, Saitama, Japan

Corresponding author: Caroline Ospelt, Center of Experimental Rheumatology, University Hospital Zurich, Gloriastrasse 23, CH-8091 Zurich, Switzerland, Tel: ++41-44-255-5866, Fax: ++41-44-255-4177, E-mail: caroline.ospelt@usz.ch

The research leading to these results has received funding from the European Community's Framework Programme FP7 Masterswitch and the Institute of Arthritis Research (IAR), Epalinges, Switzerland.

Received: May 05, 2011; Revised: Sep 14, 2011; Accepted: Nov 29, 2011

Keywords: Rheumatoid Arthritis, innate immunity, NOD1

ABSTRACT

Objective: Previously, we reported that pattern-recognition receptors (PRRs) such as TLRs and NOD2 contribute to the pathogenesis of rheumatoid arthritis (RA). Now, we analyzed the expression, regulation and function of the PRR NOD1 in RA synovial fibroblasts (RASFs) and its interaction with other PRRs.

Methods: Expression of NOD1 was analyzed by immunohistochemistry in RA, psoriasis arthritis, gout and OA synovial tissues. RASFs and monocyte-derived macrophages (MDMs) were stimulated with Tri-DAP, Pam3, PIC, LPS, heat inactivated bacteria, TNF-α or IL-1β. IL-6, CCL5, MMPs, NODs and TLRs were measured by Real-time PCR and/or ELISA. NOD1 and NOD2 were silenced with target specific siRNA. Phosphorylation of IRAK1 was measured by Western blot.

Results: In RA synovium, expression of NOD1 protein was significantly increased compared to OA synovium. There was similar basal expression of NOD1 in RASFs, OASFs, healthy controls PBMCs and MDMs. TLR3 stimulation further up-regulated NOD1 expression in RASFs. Expression of IL-6, CCL5, MMPs, TLR2 and NOD2 was significantly up-regulated in RASFs by stimulation with the NOD1 ligand. There was a synergistic effect in IL-6 production by stimulation with NOD1 and TLR2 ligands and NOD1 and TLR4 ligands. Silencing of NOD1, but not NOD2 decreased IL-6 levels after TLR2 and IL-1β stimulation and blocked phosphorylation of IRAK1.

Conclusion: NOD1 is strongly expressed in synovial tissues from RA patients in different cell types. Our data indicate that NOD1 alone and in interaction with other inflammatory activators plays an important role in the chronic and destructive joint inflammation in RA.

INTRODUCTION

Although the pathogenesis of rheumatoid arthritis (RA) remains as yet unclear, it has long been suggested that activation of the innate immune system by endogenous or exogenous stimuli contribute to its pathogenesis (1, 2). Fungal, bacterial and viral pathogens but also endogenous danger signals e.g. heat-shock proteins are recognized by specific pattern-recognition receptors, such as Toll-like receptors (TLRs) and nucleotide-binding oligomerization domain (NOD)-like receptor (NLRs). While TLRs are cell-surface or endosomal receptors, NLRs are cytosolic molecules. Both TLRs and NLRs mediate the production of proinflammatory mediators via initiation of the transcription factor NF-κB and the MAP kinase cascade (3, 4).

Recently, we have demonstrated that RA synovial fibroblasts (RASFs) express specific TLRs and the NLR NOD2, and that their activation plays a role in the pathogenesis of RA by induction of proinflammatory cytokines, chemokines, and matrix degrading enzymes (5-7). Together with NOD2, NOD1 belongs to the group of caspase-activation and recruitment domain (CARD) containing NLRs and is known to be expressed in antigen-presenting cells and epithelial cells (8, 9). It senses the peptidoglycan-related molecule diaminopimelic acid (DAP) which is a constituent of most Gram-negative bacteria and specific Gram-positive bacteria such as *Listeria* and *Bacillus spp* (10). NOD1 has been found to be crucial for host defence against a variety of bacteria including *Helicobacter pylori* and *Chlamydiae* (11, 12). Accordingly, it was shown to induce an inflammatory response in many different cell types and to synergize with TLR receptors to coordinate the immune defense (9, 13, 14). Moreover, a polymorphism in NOD1 was shown to be associated with susceptibility to chronic inflammatory diseases such as asthma and inflammatory bowel disease (15, 16).

To clarify the role of NOD1 in RA and its possible interaction with other innate immune pathways, we analyzed the expression of NOD1 in synovial tissues and synovial fibroblasts (SFs). We show expression, regulation, and function of NOD1 in synovial cells and found a

novel role of NOD1 in promoting TLR2 signaling pathways in synovial fibroblasts.

MATERIALS AND METHODS

Synovial tissues and culture of synovial fibroblasts, peripheral blood mononucleated cells (PBMCs) and monocyte-derived macrophages (MDM)

RA and osteoarthritis (OA) synovial tissues were obtained from patients undergoing joint replacement surgery (Schulthess Clinic, Zurich, Switzerland). Gout or psoriasis arthritis (PA) synovial tissues were obtained from biopsies. All patients signed a consent form before procedure and the study was permitted by the local ethical authorities. Patients with RA fulfilled the revised criteria from the American College of Rheumatology (ACR) for classification of RA (17). SFs were isolated by digestion of the synovial tissues (150 mg/ml dispase, 37°C, 60 minutes) and cultured in Dulbecco's minimum essential medium (Gibco Invitrogen, Basel, Switzerland) supplemented with 10% foetal calf serum (FCS), 50 U/ml penicillin/streptomycin, 2 mM L-glutamine, 10 mM HEPES, and 0.2% amphotericin B (all from Gibco Invitrogen). Cell cultures were maintained at 37°C in a humidified 5% CO_2 incubator. For the experiments, cultured SFs from passages 4 to 8 were used.

PBMCs were isolated from EDTA-blood of healthy donors using Ficoll-Paque PLUS gradient centrifugation. For the generation of MDMs, peripheral blood monocytes were isolated from PBMCs with CD14 MACS MicroBeads (Miltenyi Biotec, Bergisch Gladbach, Germany) and 15 ng/ml macrophage-colony stimulating factor (HumanZyme, Chicago, IL) was added every 48 hours for 7 days. MDMs and PBMCs were cultured in RPMI1640 (Gibco Invitrogen) supplemented with 10% FCS, 50 IU/ml penicillin-streptomycin, 2 mM L-glutamine, 10 mM HEPES, and 0.2% fungicide.

Immunohistochemistry/Immunofluorescence

For immunohistochemistry, sections from formalin-fixed, paraffin-embedded tissues were deparaffinised and pretreated at 80°C for 30 minutes in 10 mM citrate buffer (pH 6.0) for

antigen retrieval. After washing in H_2O, sections were incubated with 3% H_2O_2. Washing in phosphate buffered saline (PBS)/0.05% Tween was followed by 1 hour incubation in PBS/0.05% Tween/5% goat serum/1% bovine serum albumin (= blocking buffer). The sections were incubated overnight at 4°C with rabbit anti-human NOD1 antiserum (2 µg/ml; Alpha Diagnostic, San Antonio, TX). As negative control, rabbit IgG was used instead of the primary antibody. To show specificity of NOD1 antibody binding, additional antibody-blocking experiments were performed. Thereby 1 µg antibody was incubated with or without 50 µg blocking peptide (Alpha Diagnostic) at 37°C for 2 hours and then at 4 °C for 24 hours. The solutions were centrifuged for 15 minutes at 14000 rpm. Supernatants were then used as primary antibodies. After washing, all slides were incubated for 30 minutes with horseradish peroxidase (HRP)-conjugated goat anti-rabbit IgG (Jackson ImmunoResearch, Soham, UK). Antigen-antibody complexes were detected with aminoethylcarbazole chromogen substrate (DakoCytomation, Glostrup, Denmark) and counterstained with hematoxylin. The intensity of the staining was evaluated in the lining and the sublining by two observers following a gradual scale ranging from 0 (no staining) to 4 (strong staining).

For immunofluorescence double stainings, deparaffinised slides were pre-treated with 10 mM citrate buffer as described above, followed by incubation in 1 mg/ml trypsin (Sigma-Aldrich, Buchs, Switzerland) at 37°C for 20 minutes. Unspecific protein binding was blocked with blocking buffer for 1h. Slides were incubated with rabbit anti-human NOD1 antiserum plus mouse anti-human CD68 (clone PG-MA; DakoCytomation) or plus mouse anti-human vimentin (DakoCytomation) at 4°C for 24 hours (all at 2 µg/ml). 2 µg/ml rabbit IgG and mouse IgG served as negative control. Goat anti-rabbit Texas Red labeled antibodies and goat anti-mouse AlexaFluor488 labeled antibodies (both Jackson ImmunoResearch) were used as secondary antibodies. Nuclei were stained with DAPI.

Stimulation experiments

Cells were stimulated with the following agents: 10 ng/ml L-alanyl-γ-D-glutamyl-meso-

diaminopimelic acid (Tri-DAP) (InvivoGen, San Diego, CA), 10 μg/ml polyI:C (PIC) (InvivoGen), 100 ng/ml lipopolysaccharide (LPS) from *Esherichia coli* (List Biological Laboratories, Campbell, CA), 300 ng/ml palmitoyl-3-cystein-serine-lysine-4 (Pam3) (InvivoGen), 1 ng/ml interleukin-1β (IL-1β) (R&D Systems, Minneapolis, MN), 10 ng/ml tumor necrosis factor-α (TNF-α) (R&D Systems), 10^9 cells/ml heat-inactivated *Staphylococcus aureus* or heat-inactivated *Listeria monocytogenes* (InvivoGen) or 5 ng/ml polymyxin B (Sigma-Aldrich).

Quantitative Real-time polymerase chain reaction

Total RNA was isolated with the RNeasy Mini Kit (Qiagen, Basel, Switzerland) and cDNA was generated by reverse transcription using random hexamers and multiscribe reverse transcriptase (Applied Biosystems, Rotkreuz, Switzerland). Expression levels of mRNAs were determined by Taqman/SYBR Green real-time PCR on an ABI PRISM 7500 Sequence Detection System (Applied Biosystems). The sequence of primers and probes used for the detection of MMPs and TLRs are published in (7) and (6), the sequences for the SYBR primers used are as follows: **NOD1**: FORWARD gag caa agt cgt ggt caa ca; REVERSE gct gct ggg tat acc tgc tc; **NOD2:** FORWARD ttc tcc ggg ttg tga aat gt; REVERSE ctc ctc tgt gcc tga aaa gc; **IL-6:** FORWARD ctc ttc aga acg aat tga caa aca a; REVERSE gag atg ccg tcg acg atg tac; **CCL5:** FORWARD ctc ccc ata ttc ctc gga ca; REVERSE gcg ggc aat gta ggc aaa.

The expression of the housekeeping gene 18S was used as endogenous control. For calculations of fold changes, the comparative threshold cycle (Ct) method was used as previously described (6).

Silencing of NOD1

RASFs were transfected using Amaxa Basic Nucleofector kit (Lonza, Basel, Switzerland) according to the manufacturer's protocol. Briefly, cells (5 x 10^5) were resuspended in 100 μl of transfection solution, with 2.0 μg of control siRNA/NOD1 siRNA (Ambion, Austin, TX) and transfection was done using a nucleofector device (Program U23). After 24 hours of

transfection, medium was changed and cells stimulated. Silencing of NOD2 was done as previously described (18).

ELISAs

The detection of IL-6 protein in cell supernatants was performed with an OptEIA kit (BD PharMingen, San Diego, CA) according to the manufacturer's instructions. For measurements of CCL5, MMP-1 and MMP-3 DuoSet ELISA Development kits were used (R&D Systems, Minneapolis, MN).

Flow cytometry

Cells were detached with accutase (PAA laboratories, Pasching, Austria) and washed with 1% FCS in PBS. 2 µl mouse anti-human TLR2 antibodies (eBioscience, San Diego, CA) or mouse IgG2a kappa were added to 1 x 10^5 cells and incubated for 30 minutes at 4°C. After washing, cells were treated with 1 µl FITC labelled goat anti-mouse IgGs (Jackson ImmunoResearch) for 30 minutes at 4°C. Cells were washed and resuspended in 1% FCS in PBS and analyzed on a FACSCalibur flow cytometer. Data were processed using CellQuest software (BD Biosciences, Dan Diego, CA)

NOD1 protein was detected by intracellular staining using the BD Cytofix/Cytoperm kit (BD PharMingen). Permeabilized cells were incubated for 30 minutes at 4°C with 1 µg/ml of rabbit anti-human NOD1 antiserum (Alpha Diagnostic) or goat anti rabbit IgG as isotype control. Cells were washed with BD Perm/Wash solution and subsequently incubated for 30 minutes at 4°C with 0.5 µg/ml of FITC-labeled goat anti-rabbit Ig (BD PharMingen). After 2 more washing steps with BD Perm/Wash solution, cells were resuspended in 1% FCS in PBS and analyzed on a FACSCalibur flow cytometer. Data were processed using CellQuest software (BD Biosciences). To show specificity of the binding of NOD1 antibodies, antibody-blocking experiments were performed as described for immunohistochemistry. The blocking peptide blocked > 90% of NOD1 staining.

Western blotting

Whole cell lysates were dissolved in sample buffer (50mM Tris-HCl buffer pH6.8, 0.4% SDS, 10% glycerol, 1.5% β-mercaptoethanol and 0.001% bromophenol blue) and boiled at 95 °C for 3 minutes. Proteins were separated in a SDS polyacrylamide gel and transferred to nitrocellulose membranes. Membranes were blocked with 5% nonfat dry milk for 1 h at room temperature, and then incubated overnight at 4°C with rabbit anti-human phospho (Thr 209) – IRAK1 (Abcam, Cambridge, UK), mouse anti-human NOD2 (clone 2D, Santa Cruz Biotechnology, Santa Cruz, CA), mouse anti-human tubulin (SigmaAldrich), or mouse anti-human β-actin (Sigma-Aldrich) antibodies. The membranes were washed and then incubated for 45 minutes with the respective HRP-conjugated secondary antibodies. After washing, antigen-antibody complexes were detected with ECL Western Blotting kit (GE Healthcare, Buckinghamshire, UK). Protein levels were analyzed by Calibrated Densitometer (BIO-RAD, Hercules, CA).

Statistical analysis

Values are presented as the mean ± SEM. Mann-Whitney U test or Wilcoxon Singed Rank Test (paired samples) were applied to compare 2 groups. Non-parametric Friedman test followed by Dunn's multiple comparison test was used for multiple comparisons and synergistic interaction was calculated by TwoWay ANOVA with Replication. P values less than 0.05 were considered statistically significant.

RESULTS

Expression of NOD1 protein in RA and OA synovial tissues

We analyzed the expression of NOD1 in synovial tissues of patients with RA (n=9) and OA (n=6) by immunohistochemistry and found NOD1 to be strongly expressed in RA patients (Fig.1A). Scoring of NOD1 protein expression showed that in RA synovial tissues expression of NOD1 protein was significantly increased in the lining and sublining areas compared to OA synovial tissues. The addition of a synthetic NOD1-blocking peptide blocked staining by

NOD1 antibodies, proving the specificity of the staining (inset Fig. 1A).

To see which cells in the synovium express NOD1 we did double stainings for NOD1 and either the macrophage marker CD68 or vimentin as a mesenchymal cell marker. Macrophages as well as synovial fibroblasts and endothelial cells stained positive for NOD1 (Figs.1B and C).

NOD1 expression was also tested in patients with gout (n=6) and psoriasis arthritis (PA; n=4). While only one out of four PA synovial tissues expressed NOD1, all of the gout synovial tissues displayed strong staining for NOD1 (Fig.1D).

Expression and regulation of NOD1 in different cell types

We next examined expression and regulation of NOD1 in RASFs, OASFs, healthy PBMCs and MDMs. NOD1 was expressed by all the tested cells and there was no significant difference in the basal expression of NOD1 mRNA or protein in the different cell types (Fig. 2A). Stimulation experiments showed that levels of NOD1 were significantly up-regulated by the TLR3 ligand PIC in RASFs, while the NOD1 ligand Tri-DAP, the TLR2 ligand Pam3, the TLR4 ligand LPS, TNF-α or IL-1β had no effect on NOD1 transcription (Fig. 2B). In contrast, in MDMs neither NOD1 mRNA nor protein levels were changed by stimulation with any of the tested TLR ligands (Fig. 2C).

Expression of proinflammatory and matrix degrading molecules after stimulation with the NOD1 ligand

To learn more about the function of NOD1 signaling in synovial fibroblasts, we stimulated RASFs with the NOD1 ligand Tri-DAP and measured mRNA expression of the proinflammatory cytokine IL-6, the chemokine CCL5 (RANTES), matrix metalloproteinases and the PRRs TLR2, TLR3, TLR4 and NOD2. Expression of IL-6 and CCL5 mRNA was significantly up-regulated after 8h and 24h stimulation with Tri-DAP (Fig. 3A). Whereas the mean increase of IL-6 was 4 fold, levels of CCL5 were induced more than 20 fold by NOD1 activation. Also the expression of MMP-1, MMP-3, and MMP-13 mRNA was significantly

up-regulated by Tri-DAP (Fig. 3B). With a 6 fold increase MMP-1 mRNA was induced the strongest, followed by MMP-3 which was induced 5 fold and MMP-13 with a 4 fold increase after 8h. MMP-9 mRNA was increased in some RASFs after stimulation but the change did not reach statistical significance. Regarding PRRs, TLR3 and TLR4 expression was not induced by the NOD1 ligand, whereas TLR2 was 6 fold up-regulated by Tri-DAP after 8h stimulation (Fig. 3C). Also NOD2 expression was induced by NOD1 signalling, however a significant change was only seen after 24h stimulation (Fig. 3D). Increased expression of IL-6 (Fig. 4A), CCL5, MMP-1, MMP-3, TLR-2 and NOD2 after stimulation of RASFs with Tri-DAP were also confirmed on protein level (supplemental Fig. 1).

Additional time course experiments showed that stimulation of NOD1 in RASFs induced pro-inflammatory mediators and MMPs in a rapid response reaction (4h) and only at a later time point the expression of TLR2 (8h) and NOD2 (24h) were upregulated (Supplemental Fig. 2). We also looked whether stimulation with Tri-DAP can induce TLR ligands in MDMs, but no change in the expression of TLR2, TLR3 and TLR4 was seen after 24h stimulation with Tri-DAP (n=3, data not shown).

To ensure that the pro-inflammatory response seen after stimulation with Tri-DAP was not due to endotoxin contaminations we added polymyxin B which can neutralize the effect of LPS. No difference between Tri-DAP and Tri-DAP plus polymyxin B stimulated cells in the induction of IL-6 was seen, confirming an endotoxin-free preparation of the used Tri-DAP (Fig. 4A). For further confirmation that the measured effects after stimulation with Tri-DAP were solely mediated by the NOD1 receptor, we silenced expression of NOD1 with siRNA (Fig. 4B). Knock-down of the receptor indeed abolished the stimulatory effect of Tri-DAP in RASFs (Fig. 4C).

NOD1 synergizes with TLR2 and TLR4 in RASFs and promotes TLR2 and IL-1 signaling

Previously it was reported that NOD1 can synergize with TLR2 and TLR4 in the production

of IL-6 and IL-1β in human monocytes, dendritic cells and PBMCs (9, 14). To elucidate a possible crosstalk between NOD1 and TLR pathways in RASFs co-stimulation experiments with Tri-DAP and the TLR2 ligand Pam3, the TLR3 ligand PIC and the TLR4 ligand LPS were done. Similar to published results in immune cells also in RASFs, a synergistic effect of simultaneous stimulation of NOD1 with TLR2 and TLR4, but not with TLR3 was found (Fig. 5A).

Since a modulating effect of NOD1 on TLR2/NOD2 signalling pathways has been suggested in mice (19), we tested whether knock-down of NOD1 would have any influence on IL-6 production after TLR stimulation. While the absence of NOD1 did not alter the response to TLR3 or TLR4 activation, IL-6 levels were 24% lower after TLR2 stimulation when NOD1 was knocked-down, suggesting a promoting role for NOD1 in TLR2 signaling (Fig 5B). No such effect was seen when NOD2 was knocked-down, where levels of IL-6 were the same after TLR2 stimulation in control transfected cells and siNOD2 transfected cells (Fig. 5B).

We then tested whether the modulating effect of NOD1 would still be effective, if TLR2 pathways were not selectively activated, but in combination with other pattern recognition receptors. The cell wall of *Staphylococcus aureus* contains TLR2 activating peptidoglycans as well as NOD2 activating muramyl dipeptides (MDP). The cell wall of *Listeria monocytogenes* in addition contains DAP and therefore stimulates TLR2, NOD2 and NOD1 pathways. The double and triple activation of PRRs overruled the modulating effect of NOD1 seen with specific TLR2 stimulation alone and no difference in IL-6 production between NOD1 silenced and control RASFs was seen (Fig. 5C left panel). Since this specific effect of NOD1 silencing on TLR2 signaling could be due to downregulation of TLR2 itself by NOD1 silencing, we measured TLR2 transcripts after silencing of NOD1. As described before TLR2 levels were strongly increased after incubation of RASFs with TLR2 ligands, but silencing of NOD1 had no effect on TLR2 levels in unstimulated or stimulated cells (Fig. 5C right panel).

From the three TLRs analyzed TLR2 is the only one that exclusively signals via the adaptor

protein MyD88. Therefore, we hypothesized that NOD1 might influence the MyD88 signaling pathway. If this was the case, then NOD1 knock-down should diminish IL-1 signaling, since MydD88 is also recruited by the IL-1 receptor after ligand binding. Stimulation of NOD1 knocked-down cells with IL-1β led to 18% less production of IL-6 than IL-1β stimulation in control transfected cells, corroborating a modulating role of NOD1 in the MyD88 pathway (Fig. 5D).

Activation of MyD88 leads to phosphorylation of the interleukin-1 receptor-associated kinase IRAK1. Accordingly we found that stimulation of RASFs with Pam3 increased phosphorylation of IRAK1 20 min after stimulation (Fig. 6). Knock-down of NOD1 however prevented IRAK1 phosphorylation after Pam3 stimulation.

DISCUSSION

In the current study, we show that NOD1 is strongly expressed in RA synovium and that its expression can be induced in RASFs by stimulation of TLR3. NOD1 stimulation of RASFs led to a rapid increase in the production of pro-inflammatory and matrix-degrading mediators, followed by up-regulation of the expression of TLR2 and NOD2 and synergized with TLR2 and TLR4 stimulation in the production of IL-6. Finally, knock-down of NOD1 diminished IL-6 production after stimulation with Pam3 and IL-1β and blocked phosphorylation of IRAK1.

As shown in our results NOD1 expression is equally high in synovial fibroblasts, macrophages and PBMCs. Furthermore, TLR3 stimulation further increased expression of NOD1 in RASFs. The high levels of NOD1 in RA synovial tissues compared to OA synovial tissues is therefore most probably based on influx of immune cells in the synovium on the one hand, and higher NOD1 expression in RASFs caused by TLR3 activation on the other. It has been shown that endogenous double-stranded RNA from necrotic cells can activate RASFs via TLR3, which might be the mechanism by which expression of NOD1 is increased in